



An alkali-free barium borosilicate viscous sealing glass for solid oxide fuel cells



Jen-Hsien Hsu^a, Cheol-Woon Kim^b, Richard K. Brow^{a,*}, Joe Szabo^b, Ray Crouch^b, Rob Baird^b

^a Material Research Center, Missouri University of Science and Technology, Rolla, MO 65409, USA

^b Mo-Sci Corporation, 4040 HyPoint North, Rolla, MO 65401, USA

HIGHLIGHTS

- An alkali-free, barium borosilicate viscous sealing glass (G102) has been developed.
- G102 glass does not crystallize after >2000 h at SOFC operational temperatures.
- The volatilization rates and resistivities of G102 glass have been measured.
- G102 seals remain hermetic after 148 thermal cycles between 25 °C and 800 °C.
- Cracked seals created by thermal shock re-seal when reheated to 744 °C (10^{5.8} Pa-s).

ARTICLE INFO

Article history:

Received 5 June 2014

Received in revised form

13 July 2014

Accepted 15 July 2014

Available online 23 July 2014

Keywords:

Solid oxide fuel cells

Viscous sealing glass

Self-healing

Volatility

Resistivity

Interfacial reaction

ABSTRACT

An alkali-free, alkaline earth borosilicate glass (designated G102) has been developed as a viscous sealant for use with solid oxide fuel cells (SOFCs). The glass possesses the requisite viscosity, electrical resistivity, and thermal and chemical stability under SOFC operating conditions to act as a reliable sealant. Sandwich seals between aluminized stainless steel and a YSZ/NiO–YSZ bilayer survived 148 thermal cycles (800 °C to room temperature) in both oxidizing and reducing atmospheres at a differential pressure of ~3.4 kPa (0.5 psi) without failure. For sandwich seals that were held at 800 °C for up to 2280 h in air, G102 resisted crystallization, there were limited interactions at the G102/YSZ interface, but BaAl₂Si₂O₈ crystals formed at the glass/metal interface because of the reaction between the glass and the aluminized steel. Sandwich seals that were intentionally cracked by thermal shock resealed to become hermetic upon reheating to temperatures as low as 744 °C.

© 2014 Elsevier B.V. All rights reserved.

1. Introduction

Planar solid oxide fuel cells (SOFCs) are capable of achieving higher power density than tubular SOFCs, but hermetic seals are required to prevent mixing of the fuel and oxidant, and to provide electrical insulation [1,2]. It is still a challenge to develop sealing materials that retain desirable physical properties, are chemically compatible with other fuel cell components at high temperature

(e.g. 800 °C) in wide range of oxygen partial pressure, and remain operational over 40,000 h [3–5].

The most common sealing material is glass, which can be classified into rigid or compliant (viscous) seals. Glasses are inexpensive, relatively easy to incorporate into standard manufacturing processes, and have properties, like the coefficient of thermal expansion (CTE) and sealing temperatures, that can be tailored for specific applications [6–8]. Alkaline earth aluminosilicate glass-ceramics, with CTE matches to other SOFC materials, are one example of rigid seals for SOFC applications [5,9–11]. However, glass-ceramic seals are vulnerable to fracture because of thermal shock or because of thermal cycling stresses due to CTE-mismatches [12], and their failure would lead to a permanent loss of hermeticity. Compliant glass seals are designed to be viscous

* Corresponding author. Material Research Center, Missouri University of Science and Technology, 101 Straumanis-James Hall, 401 W. 16th St., Rolla, MO 65409-0330, USA. Tel.: +1 573 3416812; fax: +1 573 3416934.

E-mail address: brow@mst.edu (R.K. Brow).

under SOFC operational conditions. Stresses that might develop when a seal is thermally cycled will be relieved upon reheating [13], and cracks that might form in the seal could be “self-healed” through viscous flow [12,14].

Borate-containing glasses and glass–ceramics have been considered for SOFC sealing materials [14,15]. The addition of boron oxide to a silicate glass can decrease viscosity and sealing temperatures [5–7,16], stabilize the glass against crystallization [4,5,10], and modify CTE [6,7]. On the other hand, the formation of volatile boron-species under operating conditions may affect the long-term reliability of an SOFC [15,17].

A second issue of thermal and chemical stability involves the reactions between a sealing material and other SOFC components. In general, silicate based sealing glasses are compatible with YSZ [14,18,19], but can react with Cr_2O_3 -forming stainless steels, a common choice for the interconnect material. Alkali components in sealing glasses may react to form volatile $\text{Na}_2\text{CrO}_{4(g)}$ and $\text{K}_2\text{CrO}_{4(g)}$, which causes Cr to deposit on the cathode, blocking active sites [4,20,21]. Under oxidizing conditions, alkaline earth silicate glasses can react with interconnects to form deleterious high expansion chromates, i.e. BaCrO_4 ($\text{CTE} > 16 \times 10^{-6} \text{ }^\circ\text{C}^{-1}$) [22] and SrCrO_4 ($\text{CTE} \sim 22 \times 10^{-6} \text{ }^\circ\text{C}^{-1}$) [23]. Also, the electrical resistivity of a sealing glass drops when iron from the interconnect dissolves into the glass [24]. Alumina protective coatings on stainless steel have been developed that prevent the formation of deleterious chromates [25,26]. However, several studies have shown that sealing glasses can react with aluminized steel to form $\text{BaAl}_2\text{Si}_2\text{O}_8$ crystals at the glass/metal interface [3,14,19].

In a previous work [14], an alkali-free borosilicate glass, G73, was developed for compliant seals for SOFCs. These seals remained hermetic over 100 thermal cycles ($750 \text{ }^\circ\text{C}$ to room temperature) in dry air and wet forming gas at a differential pressure of $\sim 3.4 \text{ kPa}$ (0.5 psi). Seals that were deliberately cracked by thermal shock were successfully re-sealed upon reheating to temperatures as low as $700 \text{ }^\circ\text{C}$. To the authors' knowledge, this was the first report of “self-healing” for a prototype SOFC seal. However, G73 slowly crystallized with time and the resulting increase in seal viscosity would degrade this “self-healing” characteristic.

In the present paper, an alkali-free borosilicate viscous SOFC sealing glass (G102) is described. The glass is a modified version of G73 and exhibits no evidence for crystallization after $>2200 \text{ h}$ at $800 \text{ }^\circ\text{C}$. Glass properties and the long-term stability of seals made between G102 and SOFC components are reported. Finally, “self-healing” of thermally shocked G102 seals is demonstrated.

2. Experimental procedures

2.1. Glass formulation and properties

The glass used in this study, designated G102, is an alkaline earth aluminoborosilicate with 45 mol% B_2O_3 and 24 mol% SiO_2 . A homogeneous mixture of the appropriate raw materials was melted in a silica crucible (99.6% SiO_2 , 0.2% Al_2O_3) at $1100 \text{ }^\circ\text{C}$ for 4 h in air, then quenched onto a clean steel plate and annealed.

The CTE ($40\text{--}500 \text{ }^\circ\text{C}$) and glass transition temperature (T_g) were determined by dilatometry (Orton 2012 STD) in air at $5 \text{ }^\circ\text{C min}^{-1}$. Differential thermal analysis (DTA, Perkin–Elmer Analysis TAC 7/DX) was done with about 32 mg of G102 powder ($<106 \mu\text{m}$) heated in a Pt crucible under nitrogen at a rate of $10 \text{ }^\circ\text{C min}^{-1}$ up to $1000 \text{ }^\circ\text{C}$. The liquidus temperature (T_L) was determined following ASTM C829–81 [27]. A platinum boat was filled with the G102 powder ($<180 \mu\text{m}$), then heated in air for 72 h in a gradient furnace set to cover the temperature range from $657 \text{ }^\circ\text{C}$ to $850 \text{ }^\circ\text{C}$. After the heat treatment, the glass surface and cross-section were observed using optical microscopy (Hirox KH-8700) and scanning electron

microscopy (Helios NanoLab 600 FIB/FESEM) with energy dispersive spectroscopy (EDS). The microscopy specimens were prepared using normal metallography procedures.

The high temperature melt viscosity was measured using the rotating spindle technique [28] with a high temperature viscometer (Haake ME 1700). About 60 g of crushed G102 was re-melted in a platinum crucible in the viscometer at $1050 \text{ }^\circ\text{C}$ for 2 h to remove bubbles from the melt. The platinum spindle was then lowered into the melt and rotated at the designated speed. The furnace was cooled to $750 \text{ }^\circ\text{C}$ at an average rate of $10 \text{ }^\circ\text{C min}^{-1}$. The torque required to maintain the spindle speed was recorded and used to calculate the melt viscosity. The process was repeated twice and the average results are reported.

In the softening range ($10^4\text{--}10^8 \text{ Pa s}$), the viscosity was determined by using the parallel plate method [29] with a dynamic-mechanical analyzer (DMA, Perkin–Elmer DMA-7). A cylinder of G102 with a diameter of 5 mm and a height of 5 mm was core-drilled from an annealed bulk glass sample. The viscosity values were obtained by applying a static force (2000 mN) to the cylinder and measuring the deformation rate at a constant heating rate ($5 \text{ }^\circ\text{C min}^{-1}$) [29]. The process was repeated twice and the average results are reported.

Glass stability against volatilization was determined by measuring weight loss in air with time (up to 2000 h) at designated temperatures. Platinum boats were loaded with G102 powders ($<106 \mu\text{m}$) and held at $650 \text{ }^\circ\text{C}$ and $750 \text{ }^\circ\text{C}$. The weights of those Pt boats were periodically measured and normalized weight losses (per unit surface area) were recorded. After the tests, glass samples were mounted in epoxy, cut in half to microscopically observe their cross-sections. Other samples were ground to powders ($<150 \mu\text{m}$) and analyzed using X-ray diffraction (Philips X-Pert Diffractometer).

Electrical resistance measurements were made using a procedure similar to that described in Refs. [30], using aluminized stainless steel (Al-SS441) coupons supplied by Pacific Northwest National Laboratory (PNNL). G102 powders ($<106 \mu\text{m}$) were sandwiched between two Al-SS441 plates ($50 \text{ mm} \times 50 \text{ mm} \times 1 \text{ mm}$) without any binder and then heated at $850 \text{ }^\circ\text{C}$ for 8 h to create a sandwich seal. An external DC voltage of 0.8 V was then applied to the sandwich seal with a commercial power supply (Agilent E3632A) and the current flowing through the circuit was calculated by measuring the voltage drop of a resistor in parallel with the sample, and the resistivity of the glass, normalized to thickness and surface area, was measured, at $650 \text{ }^\circ\text{C}$ and $750 \text{ }^\circ\text{C}$.

2.2. Hermetic seals and interfacial reactions

Hermetic seals were made with G102 glass between a washer of aluminized SS441 and a YSZ/NiO–YSZ bilayer provided by PNNL, using a process similar to that used to prepare the electrical resistivity samples. These samples were then assembled in a test chamber where they could be heated in different atmospheres with a differential pressure ($\sim 3.4 \text{ kPa}$) across the seal. This system is similar to those used in other studies of SOFC glass seals [3,12]. The seals were heated ($\sim 13 \text{ }^\circ\text{C min}^{-1}$) to $800 \text{ }^\circ\text{C}$, held 1 h, then cooled ($\sim 5 \text{ }^\circ\text{C min}^{-1}$) to room temperature, in either air or wet forming gas (5% H_2 and 95% N_2 bubble through $70 \text{ }^\circ\text{C}$ DI-water with a flow rate of 10 ml s^{-1}). Samples were continuously thermally cycled between $800 \text{ }^\circ\text{C}$ and room temperature, and the differential pressure across the seal was monitored. Upon the completion of these tests, the sandwich seal assemblies were analyzed by analytical scanning electron microscopy, using the procedures and equipment noted above.

Sandwich seals between Al-SS441 washers and YSZ/NiO–YSZ bilayers were also used in re-sealing tests. The glass in these seals were deliberately cracked by removing the assembly from a furnace

Table 1
Properties, viscosity fitting parameters and isokom temperatures for G102.

| Dilatometry data | | Viscosity (MYEGA) fitting parameters | | Isokom temp. (°C), log η (Pa s) | | | | | |
|------------------|-------------------------------------|--------------------------------------|------------|--------------------------------------|-----|-----|-----|-----|-----|
| T_g (°C) | CTE (40–500 °C) | m | T_g (°C) | log η_∞ (Pa s) | 11 | 9 | 6.6 | 4 | 2 |
| 603 | $73 \times 10^{-7} \text{ °C}^{-1}$ | 57.2 | 593 | −3.3 | 610 | 647 | 706 | 800 | 916 |

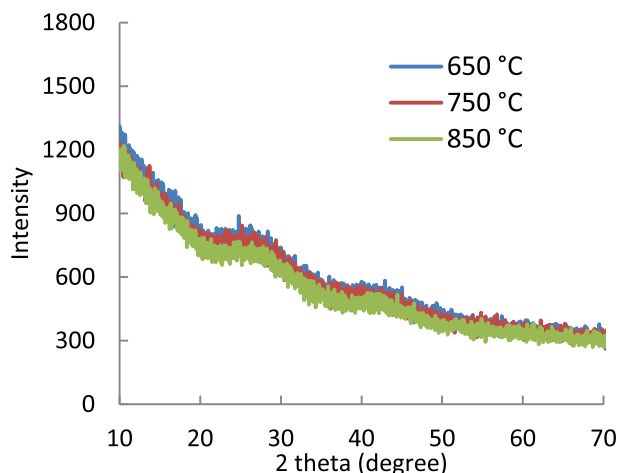


Fig. 1. XRD patterns of G102 after 2184 h at 650 °C, 750 °C and 850 °C.

at 800 °C and applying drops of water to the steel to thermally shock the glass. Visible cracks in the glass layer were noted and confirmed by the flow of nitrogen (up to 13.8 kPa) through the crack. Cracked seals were then reheated to a designated temperature for 2 h, then slowly cooled to room temperature where hermeticity was determined.

Additional sandwich seal samples were prepared to characterize the long-term interfacial reactions between the sealing glass and SOFC components, using materials and techniques similar to those used to prepare the hermeticity samples. These reaction couples were held in air at 800 °C for up to 95 days, and then analyzed by analytical electron microscopy. In this report, the YSZ/NiO–YSZ bilayer was always on the top in the furnace during the isothermal heat treatments.

3. Results and discussion

G73 is an alkali-free borosilicate glass that exhibited “self-healing” behavior when sealed between Al-SS441 and YSZ/NiO–YSZ bilayers [14]. After 2000 h at 800 °C, however, barium silicate crystals could be detected in the glass. Analyses of the residual glass

between these crystals guided the development of G102. In general, the new glass has a lower alkaline earth content and a greater silica content than does G73.

3.1. Thermal properties and characteristic temperatures

Table 1 shows the CTE and T_g of G102 from the dilatometry data. DTA (not shown) shows no evidence for crystallization. No crystals could be detected in the G102 sample, held for 72 h in the gradient furnace between 657 °C and 850 °C according to ASTM C829–81, indicating unusually slow crystallization kinetics for this glass in this temperature range. In fact, samples isothermally held for ~2200 h in a platinum crucible in air at temperatures at 650 °C, 750 °C and 850 °C remained x-ray amorphous (Fig. 1).

In order to promote crystallization, G102 powders, in a platinum boat, were thermally cycled 84 times (over 21 days) between 610 °C and 800 °C, heating and cooling at 1.2 °C min^{-1} with 22 min holds at each temperature. Fig. 2(a) shows that the glass near the wall of the platinum boat turned cloudy, and optical microscope images of this cloudy region reveal the presence of crystals (Fig. 2(b)), which are identified by XRD to be hexagonal $\text{BaAl}_2\text{Si}_2\text{O}_8$. The micrograph of the cross-section of the cloudy (crystallized) area (Fig. 2(c)) reveals that only surface crystals are present; there is no evidence for bulk crystallization.

The surface crystallized G102 sample was then isothermally heated for 30 min to progressively higher temperatures and examined by optical microscopy until the crystals dissolved. Based on these experiments, the liquidus temperature of G102 is between 866 °C and 868 °C.

3.2. Viscosity

Fig. 3 shows the viscosity-temperature data for G102, including the intermediate temperature values measured by the parallel plate technique and the high temperature values measured by the rotating spindle technique, with their fit to the MYEGA viscosity model [31]. Table 1 summarizes the fitting parameters of the MYEGA model for G102 and indicates several important isokom temperatures based on the viscosity model. The Littleton softening point ($\log \eta$ (Pa s) = 6.6) is sometimes described as the temperature at which a glass flows under its own weight [32] and this is predicted for G102 to be at ~706 °C. Thus, G102 should be viscous at SOFC operational temperatures. It is worth noting that the T_g measured by dilatometry (603 °C) is in good agreement with the T_g from the viscosity data (593 °C, defined as $\log \eta = 12$ (Pa s)). Finally, the intermediate range viscosity of a sample that was held for 2000 h at 800 °C in an alumina crucible was unchanged from that of the original glass (Fig. 3), indicating that the viscous properties of this glass are stable with time, a desirable characteristic for a reliable sealant.

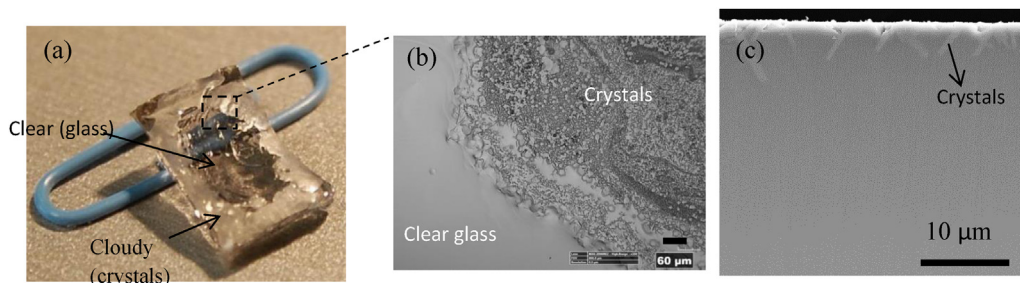


Fig. 2. (a) Appearance and (b) surface micrograph (c) the cross-section of the cloudy area of the G102 sample under thermal cycles (610–800 °C) for 21 days in Pt boat in air. Image(b) is a high magnification view of the area in the dashed box in image(a).

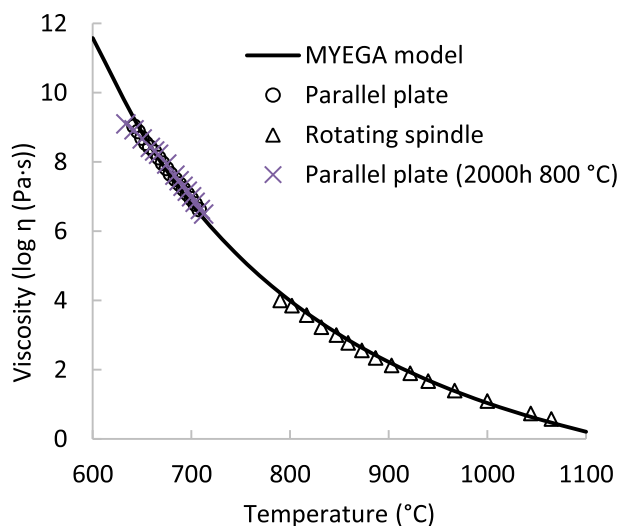


Fig. 3. Viscosity data (symbols) for G102 fit with the MYEGA model (solid line).

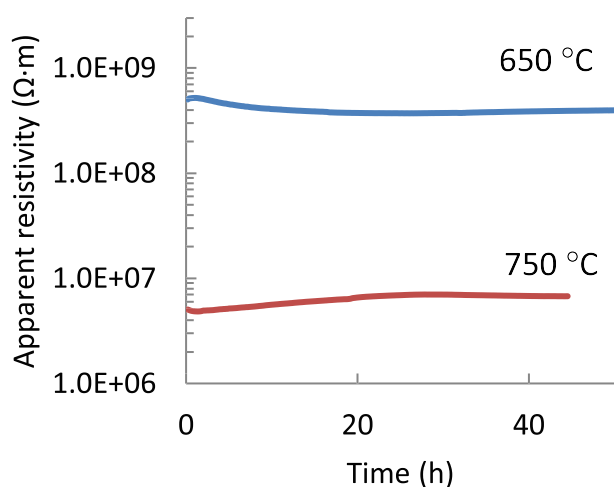


Fig. 4. Resistivity measurement of G102 at 650 °C and 750 °C.

3.3. Electrical resistivity

The resistivity measured in the present study combines the resistivity of the sealing glass with those of the two Al-SS441 plates and the two sets of interfacial oxides. Because of uncertainties associated with the latter, “apparent” resistivity was adopted, consistent with other researchers using a similar experimental setup [18,30].

The apparent resistivity of G102, measured at 650 °C and 750 °C in air, remained relatively constant at $\sim 4 \times 10^8 \Omega \cdot \text{m}$ and $\sim 7 \times 10^6 \Omega \cdot \text{m}$, respectively, over the two days of continuous testing (Fig. 4). These values are several orders of magnitude greater than those reported for other glass and glass-ceramics materials tested under similar conditions [18,24,25].

3.4. Volatility

Changes in the weight of G102 glass held in a Pt boat at 650 °C and 750 °C for 2000 h in air produced average volatility rates of $7 \times 10^{-10} \text{ g mm}^{-2} \text{ h}^{-1}$ and $5 \times 10^{-9} \text{ g mm}^{-2} \text{ h}^{-1}$, respectively. These values are comparable to other SOFC sealing glasses; e.g. $1.6 \times 10^{-9} \text{ g mm}^{-2} \text{ h}^{-1}$ [33] and $3.6 \times 10^{-10} \text{ g mm}^{-2} \text{ h}^{-1}$ [34] for borosilicate glasses in wet forming gas at 780 °C and 800 °C, respectively; 1×10^{-9} – $8 \times 10^{-9} \text{ g mm}^{-2} \text{ h}^{-1}$ for a borate-free alkali silicate glass at 800 °C in air or wet forming gas [35]; and $1.7 \times 10^{-8} \text{ g mm}^{-2} \text{ h}^{-1}$ (750 °C, dry air) and $2.0 \times 10^{-8} \text{ g mm}^{-2} \text{ h}^{-1}$ (750 °C, wet forming gas) for G73 [14].

3.5. Interfacial reactions

SOFC reaction couples were prepared to characterize the long-term interactions between G102 and other SOFC materials. Fig. 5 shows representative images at different magnifications of a reaction couple held at 800 °C for 95 days in air. The glass layer cracked horizontally during the preparation of the cross-sections, and the epoxy that was used to mount the samples filled the gap. No evidence for significant crystallization is evident either in the bulk of the glass or near the glass/YSZ interface (Fig. 5(b)). EDS-linescans (Fig. 6(a) and (b)) indicate that the glass is compositionally uniform and that no elements have diffused from either the SS441 (i.e. Fe and Cr) or YSZ (i.e. Y, Zr) into the glass.

Crystals do form near the glass/Al-SS441 interface (Fig. 5(c)), and EDS analyses indicate that they have a stoichiometry close to $\text{BaAl}_2\text{Si}_2\text{O}_8$. This is consistent with an experiment, described in Refs. [19], where powders of G73 and alumina (99.5%) were

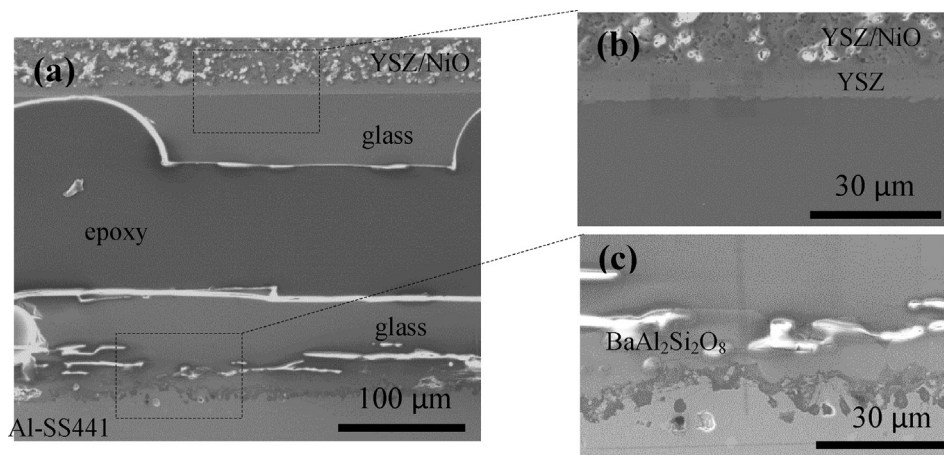


Fig. 5. Cross-section micrograph of a sandwich seal after 95 days (2280 h) at 800 °C in air. Image(b) and (c) is a high magnification view of the area in the dashed box in image(a).

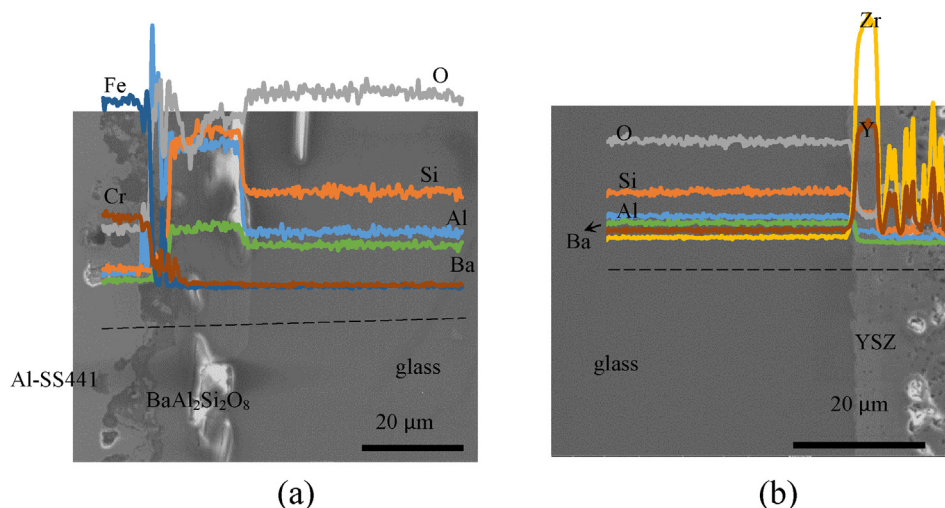


Fig. 6. EDS line-scans at (a) glass/Al-SS441 interface (b) glass/YSZ interface of the G102 sandwich seals after 95 days at 800 °C in dry air. The dash line indicates the scan area.

uniformly mixed using a 1:1 weight ratio, heat-treated at 800 °C for 500 h and then analyzed using XRD, producing the monoclinic and hexagonal phases of $\text{BaAl}_2\text{Si}_2\text{O}_8$.

In a previous study [19], it was shown that Al diffuses preferentially from the aluminized layer on SS441 into the adjacent sealing glass to form $\text{BaAl}_2\text{Si}_2\text{O}_8$ crystals, and a similar reaction is occurring here. Fig. 7 compares the Al-concentration gradients, measured by EDS (solid symbols), of the as-received Al-SS441 sub-surface with the Al diffusion depth profiles at both the air-side and the glass-side interfaces after different heat treatment times. The more rapid depletion of Al at the glass-side interface implies that Al is not diffusing deeper into the metal as it is at the air-side, but instead is preferentially diffusing from the metal into the glass. There is no evidence for a retreat of the metal surface at either interface. If the Al-rich region dissolved into the glass, large concentrations of Fe and Cr should also be present, and this was not

observed in the EDS scans (Fig. 6(a)). Because there is no significant oxide growth on the air-side of the Al-SS441, even after 95 days at 800 °C, the changes in the Al-concentration gradients of the Al-SS441 sub-surface on the air-side are assumed to result from Al diffusion from the sub-surface into the metal matrix. The calculated diffusion profiles (lines) are in reasonable agreement with the air-side experimental results (solid symbols) (Fig. 7). The details of the Al diffusion calculations are reported in Ref. [19].

3.6. Hermetic sealing tests

Fig. 8 shows some results from the thermal cycling tests of sandwich seals made with G102. A constant differential pressure (~3.4 kPa) was maintained across the seal after 148 thermal cycles between room temperature and 800 °C in air, over the course of ~5020 h; similar results were obtained for a seal tested at 800 °C in wet forming gas. These tests were terminated after 148 thermal cycles to examine the sealed interfaces.

Fig. 9(a) and (b) show SEM images of the seals from the thermally cycled samples run in air and wet forming gas, respectively. The samples are similar to each other and to sandwich seals from the isothermal experiments. There is no evidence for crystals in the

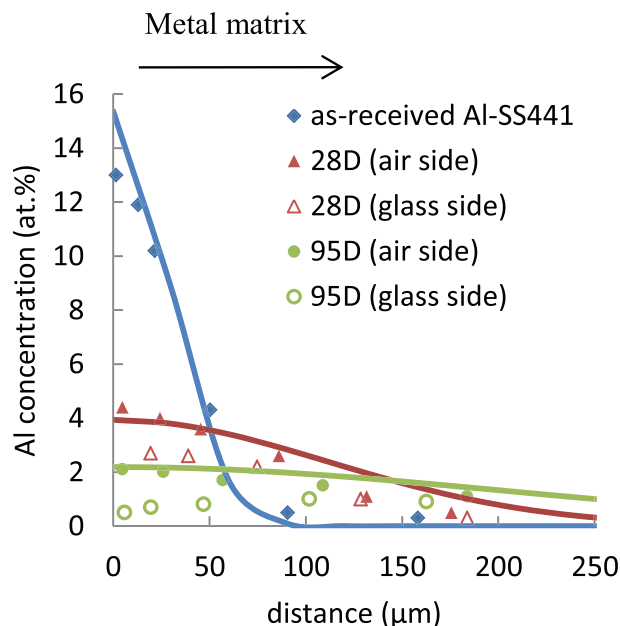


Fig. 7. Measured (symbols) and calculated (solid lines, see Ref. [19]) aluminum diffusion profiles from metal surfaces on the air-side and glass-side for the SOFC reaction couples held at 800 °C in air for different times.

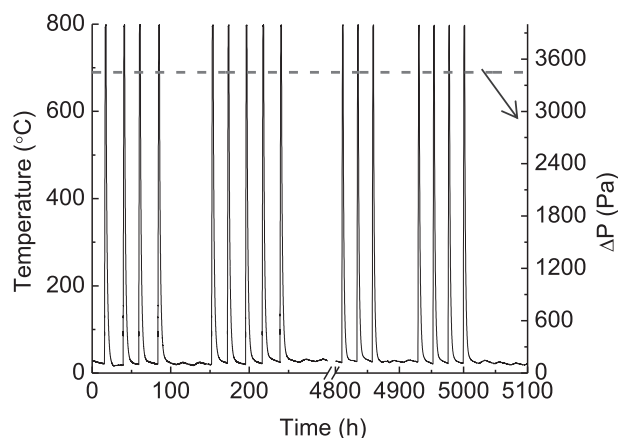


Fig. 8. Demonstration of the hermeticity of the sandwich seal assembly. This seal has survived 148 thermal cycles (800 °C to RT) in dry air at a differential pressure of ~3.4 kPa (dash line) over the course of more than 5000 h.

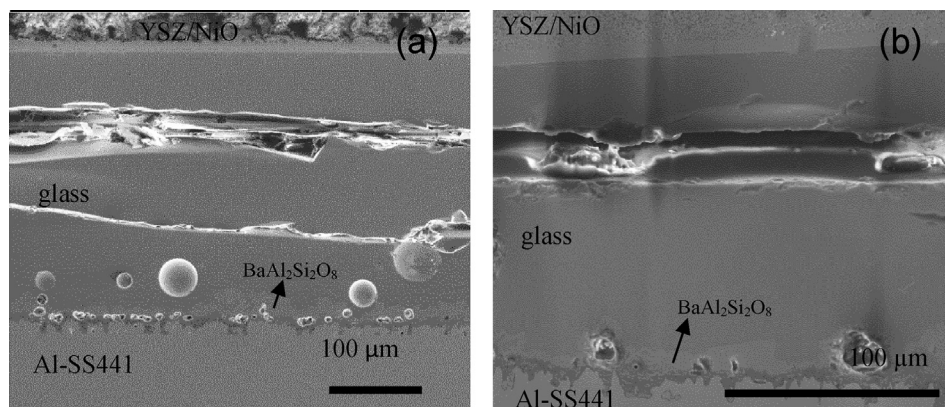


Fig. 9. Micrograph of the G102 sandwich seals that remained hermetic after 148 thermal cycles (800 °C to RT) in (a) dry air and (b) wet forming gas. The cracks in the images were formed during the preparation of the cross-sections.

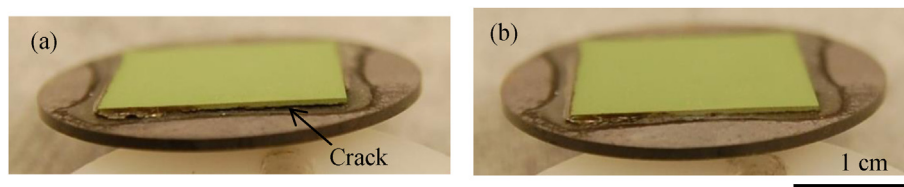


Fig. 10. Sandwich seal made with G102; (a) crack caused by thermal shock (b) crack healed and the seal was again hermetic, holding a 13.8 kPa different pressure, after re-heating at 800 °C for 2 h.

glass layers or at the interfaces with YSZ, but there are crystals at the interfaces with the Al-SS441. These crystals have morphologies similar to the crystals in the isothermal sandwich seals, and EDS analyses indicate that the crystals have the stoichiometry of $\text{BaAl}_2\text{Si}_2\text{O}_8$.

3.7. Crack healing tests

In the operation of an SOFC, cracking of the glass seal by temperature cycling or CTE mismatch is of concern. Crack healing through viscous flow is commonly observed in glass at elevated temperatures and is one important reason why viscous glasses are being considered for SOFC sealing materials [12–14]. Fig. 10(a) shows a crack formed in a G102 sandwich seal assembly after deliberate thermal shock from 800 °C. This cracked sandwich seal assembly was re-heated to 800 °C for 2 h and slowly cooled back to room temperature (Fig. 10(b)), where it was found to be once again hermetic. Fractured G102 seals were successfully resealed to temperatures as low as 744 °C, equivalent to a glass viscosity of $10^{5.8}$ Pa·s. This is similar to the minimum “self-healing” viscosity found for G73 using a similar sealing configuration [14]. The results are also consistent with the observation that the crack-healing rate of a viscous glass is directly dependent on viscosity and that crack-healing is rapid near the glass softening temperature [12].

4. Conclusions

An alkali-free borosilicate glass, designated G102, has been developed for sealing solid oxide fuel cells. The glass is viscous under SOFC operational conditions, with a glass transition temperature of 603 °C and a viscosity near 10^4 Pa·s at 800 °C. The glass showed no evidence for significant crystallization after ~2200 h at 650 °C, 750 °C and 850 °C and its viscosity did not change after 2000 h at 800 °C.

No significant crystallization was detected in G102 layers in sandwich seals with Al-SS441 and YSZ/NiO–YSZ bilayers, held at 800 °C for up to 2280 h. There was no evidence for the diffusion of Fe and Cr from the Al-SS441 or Y and Zr from the YSZ into the glass. Al is depleted from the Al-SS441 into the glass, and crystals, most likely $\text{BaAl}_2\text{Si}_2\text{O}_8$, do form at the glass/Al-SS441 interface.

G102 sandwich seals remain hermetic after 148 thermal cycles (between 800 °C and RT) in both dry air and wet forming gas. Based on SEM analyses of the cross-sections of these seals, no significant differences were observed between the sandwich seals tested in dry air and wet forming gas. The bulk glass remained crystal-free and compositionally uniform. The interfacial reactions are similar to those of sandwich seals held at 800 °C.

Self-healing of deliberately cracked G102 seals was demonstrated after reheating the seal for 2 h at temperatures as low as 744 °C in air.

Acknowledgment

The authors would like to thank Yeong-Shyung Chou and Jeffery W. Stevenson at PNNL for providing the aluminized SS441 substrates and the YSZ/NiO–YSZ bilayers, and Eric Bohannon, Charmayne Smith and Kathryn Goetschius at Missouri S&T for XRD analyses. This work was supported by the US Department of Energy under Contract # DE-SC0002491.

References

- [1] S.C. Singhal, *Solid State Ionics* 152–153 (2002) 405–410.
- [2] J.W. Kim, A. Virkar, K.-Z. Fung, K. Mehta, S.C. Singhal, *J. Electrochem. Soc.* 146 (1999) 69–78.
- [3] K.D. Meinhardt, D.-S. Kim, Y.-S. Chou, K.S. Weil, *J. Power Sources* 182 (2008) 188–196.
- [4] N. Lahl, L. Singheiser, K. Hilpert, *Electrochem. Soc. Proc.* 99-19 (1999) 1057–1066.
- [5] J.W. Fergus, *J. Power Sources* 147 (2005) 46–57.

- [6] K.L. Ley, M. Krumpelt, R. Kumar, J.H. Meiser, I. Bloom, J. Mater. Res. 11 (1996) 1489–1493.
- [7] S.-B. Sohn, S.-Y. Choi, G.-H. Kim, H.-S. Song, G.-D. Kim, J. Non Cryst. Solids 297 (2002) 103–112.
- [8] P.A. Lessing, J. Mater. Sci. 42 (2007) 3465–3476.
- [9] K.D. Meinhardt, J.D. Vienna, T.R. Armstrong, L.R. Pederson, U.S. Patent No. 6430966, 2002.
- [10] N. Lahl, K. Singh, L. Singheiser, K. Hilpert, J. Mater. Sci. 35 (2000) 3089–3096.
- [11] S.T. Reis, R.K. Brow, J. Mater. Eng. Perform. 15 (2006) 410–413.
- [12] R.N. Singh, J. Mater. Res. 27 (2012) 2055–2061.
- [13] N. Govindaraju, W.N. Liu, X. Sun, P. Singh, R.N. Singh, J. Power Sources 190 (2009) 476–484.
- [14] C.W. Kim, J.H. Hsu, C. Townsend, J. Szabo, R. Crouch, R. Baird, R.K. Brow, in: Proceedings of the Ceramic Engineering Science Advances in Solid Oxide Fuel Cells IX, vol. 34, 2013, pp. 123–132.
- [15] T. Zhang, W.G. Fahrenholtz, S.T. Reis, R.K. Brow, J. Am. Ceram. Soc. 91 (2008) 2564–2569.
- [16] R. Zheng, S.R. Wang, H.W. Nie, T.-L. Wen, J. Power Sources 128 (2004) 165–172.
- [17] C. Gunther, G. Hofer, W. Kleinlein, in: Proceedings of the 5th International Symposium on Solid Oxide Fuel Cells, vol. 97, 1997, pp. 746–756.
- [18] Y.-S. Chou, E.C. Thomsen, J.-P. Choi, J.W. Stevenson, J. Power Sources 202 (2012) 149–156.
- [19] J.-H. Hsu, C.-W. Kim, R.K. Brow, J. Power Sources 250 (2014) 236–241.
- [20] K. Hilpert, D. Das, M. Miller, D.H. Peck, R. Wei, J. Electrochem. Soc. 143 (1996) 3642–3647.
- [21] K. Ogasawara, H. Kameda, Y. Matsuzaki, T. Sakurai, T. Uehara, A. Toji, N. Sakai, K. Yamaji, T. Horita, H. Yokokawa, J. Electrochem. Soc. 154 (2007) B657–B663.
- [22] Z. Yang, J.W. Stevenson, K.D. Meinhardt, Solid State Ionics 160 (2003) 213–225.
- [23] Y.-S. Chou, J.W. Stevenson, P. Singh, J. Power Sources 184 (2008) 238–244.
- [24] Y.-S. Chou, J.W. Stevenson, K.D. Meinhardt, J. Am. Ceram. Soc. 93 (2010) 618–623.
- [25] Y.-S. Chou, J.-P. Choi, J.W. Stevenson, Int. J. Hydrogen Energy 37 (2012) 18372–18380.
- [26] Y.-S. Chou, E.C. Thomsen, R.T. Williams, J.-P. Choi, N.L. Canfield, J.F. Bonnett, J.W. Stevenson, A. Shyam, E. Lara-Curzio, J. Power Sources 196 (2011) 2709–2716.
- [27] American Society for Testing and Materials C829-81, Standard Practices for Measurement of Liquidus Temperature of Glass by the Gradient Furnace Method.
- [28] American Society for Testing and Materials C965-96, Standard Practices for Measuring Viscosity of Glass Above the Softening Point.
- [29] American Society for Testing and Materials C1351M-96, Standard Test Method for Measurement of Viscosity of Glass between 104 Pa s and 108 Pa s by Viscous Compression of a Solid Right Cylinder.
- [30] V.A.C. Haanappel, V. Shemet, S.M. Gross, Th Koppitz, N.H. Menzler, M. Zahid, W.J. Quadackers, J. Power Sources 150 (2005) 86–100.
- [31] J.C. Mauroa, Y.-Z. Yueb, A.J. Ellisona, P.K. Gupta, D.C. Allana, Proc. Natl. Acad. Sci. U.S.A. 106 (2009) 19780–19784.
- [32] J.T. Littleton, J. Soc. Glass Technol. 24 (1940) 176–185.
- [33] T. Zhang, Q. Zou, J. Eur. Ceram. Soc. 32 (2012) 4009–4013.
- [34] Y.-S. Chou, J.W. Stevenson, Refractory Glass Seals for SOFC, 2011. PNNL-20545.
- [35] Y.-S. Chou, E. Thomsen, J.-P. Choi, W. Voldrich, J.W. Stevenson, in: 12th Annual SECA Workshop, Pittsburgh, 2011.